Teknomekanik
Vol.4, No.2, Dec 2021, pp. 97~110
e-ISSN: 2621-8720 p-ISSN: 2621-9980

Utilization of Sewage Sludge Using Multiple Thermal Conversion Processes

Ta-Hui Lin[1,2], Annas Fauzy[1], Guang-Bang Chen[2], Fang-Hsien Wu[2]

[1] Department of Mechanical Engineering, National Cheng Kung University, Tainan 701, Taiwan ROC
[2] Research Center for Energy Technology and Strategy, National Cheng Kung University, Tainan 701, Taiwan ROC

Article Info

Article history:

Received Sep 09th, 2021
Revised Nov 11th, 2021
Accepted Dec 27th, 2021

Keywords:

Sewage sludge
Palm kernel shell (PKS)
Sludge pyrolytic oil (SPO)
Combustion
Co-gasification

ABSTRACT

Sewage sludge is a usual waste from urban areas that can be utilized in many renewable energy sources. In this study, we examine the sewage sludge utilization using pyrolysis process to produce pyrolytic oil using Taguchi methods, combustion characteristic of sludge pyrolytic oil (SPO) blend with heavy fuel oil (HFO), and co-gasification of sewage sludge with CO_2/steam as the gasification medium using Taguchi methods. The best-operating conditions for the pyrolysis of sewage sludge are a heating rate of 10°C/min, temperature of 450°C, the residence time of 60 min, and N_2 flow rate of 700 mL/min. Under these conditions, the obtained pyrolytic oil yield is very close to the result from the Taguchi method calculation. In the combustion characteristic of sludge pyrolytic oil (SPO) blend with heavy fuel oil (HFO), a higher SPO in the fuel blend enhances the occurrence of micro-explosion and reduces the size of the residual. Higher SPO content in the fuel blend increases the combustion rate and increases the ignition delay due to moisture evaporation. In the co-gasification of sewage sludge and palm kernel shell optimization using Taguchi method, the best operational condition for maximum H_2/ CO syngas ratio reaches at the gasification temperature of 900 C, a blending ratio of 30%, a $CO_2/(CO_2+H_2O)$ ratio of 70%, and a catalyst addition of 20% bed material mass. The best operating condition for maximum concentration of H_2 reach with gasification temperature of 800 C, a blending ratio of 40%, a $CO_2/(CO_2+H_2O)$ ratio of 70%, and a 15% catalyst addition of bed material mass. The $CO_2/(CO_2+H_2O)$ ratio is the most important parameter among both case.

Corresponding Author:

Ta-Hui Lin,
Department of Mechanical Engineering, National Cheng Kung University,
University Road, Tainan 701, Taiwan ROC
Email: thlin@mail.ncku.edu.tw

1. INTRODUCTION

Nowadays, the main energy resources still have a huge dependency from the fossil fuels. This dependency may cause the significant consumption of fossil fuel, also it has a huge effect in the production of green house effect which leads to the climate change in the future. Therefore, it is necessary to improve the renewable energy utilization efficiency to make renewable energy become sustainable to replace the fossil fuel dependency [1]–[4]. Biomass is one of promising fuel to replace the fossil fuel due some advantages such as huge abundance, environmentally friendly, and low cost. The biomass mainly produced from forestry residual, biological waste, agricultural waste, municipal waste, and many other wastes. Among those example of waste, municipal waste become a promising source of biomass due to its availability. Sewage sludge is a major municipal waste that has a complex element such as organic materials, inorganic materials, and moisture. The usual treatment of sewage sludge utilization is use in agricultural, incineration, and landfill gas production. However, this strategy has some inadequacy, for example, in the utilization of sewage sludge in the agricultural field may cause the harm for human healthy due to the contain of viruses, bacteria or parasitic microbes in the sewage sludge. For incineration, the sewage sludge heating value is categorized as low. For sewage sludge

utilization in landfill gas, the cost of this process become increase due to the requirement of a lot of area. With this lack of usual sewage sludge utilization problem, it is necessary to find a new way to utilize the sewage sludge effectively. Thermochemical process such as pyrolysis and gasification comes to this problem as a solution the sewage sludge problem [5]. Thermochemical process will be used to maximize the potency of sewage sludge as replacement of fossil duel in the future.

Pyrolysis can be considered an effective process to convert the biomass/waste into a more beneficial product. Al-Salem et al. investigate the pyrolysis process to produce a valuable oil and gas from the plastic waste[6]. Many studies have been done recently to do the sewage sludge utilization using pyrolysis [7] or the blend the sewage sludge with another biomass during the pyrolysis process [8]. Microwave-assisted pyrolysis is a promising technique to apply in sewage sludge because it is efficient in-process and time [9]. Pyrolysis lowers the sewage sludge up to 50% by volume, distils the toxic and heavy metals into char, and stabilizes the organic matter [10]. The char from the previous pyrolysis can be used as an adsorbent material for the contaminants or a reducer in metallurgic processes [11].

Evaporation and droplet combustion have an important role in industrial applications such as drying and Internal combustion engines. There are several steps that must be carried out during the combustion of droplet such as heating, gasification, and combustion. The d square (d^2) law is one of basic laws in the fuel droplet experiment proposed by Spalding [12], The d square law shows the relation between the droplet radius reduction linear with the period of droplet heating. The combustion or gasification rates of a droplets indicated by the slope of droplet size reduction with respect to the period of droplet heating.

The gasification is a process to convert a various biomass into syngas or synthesis gas which mainly contain CO, H_2, and CH_4. As a result of the gasification process, sulfur and nitrogen pollutants including H_2S, COS, NH_3, and HCN are produced [13]. Sludge gasification has several advantages, including (1) high efficiency of energy recovery, (2) environmental pollution reduction, (3) take a control majority of inorganic compounds, (4) take care of heavy metals compounds, (5) the ability to produce liquid fuel from syngas, and (6) autonomous technology [14], [15].

During the gasification process, the moisture properties of sewage sludge and its high ash content will make feeding difficult, lower the density of syngas, and cause the furnace to sinter or sludge easily. To improve the gasification of sewage sludge, many researchers do the co-gasification which is the gasification process to combine between two or more biomass during its process. A higher hydrogen and carbon monoxide composition in the syngas will obtained from the co-gasification of sewage sludge with some forest waste instead from a pure sewage sludge gasification. Another advantage in the co-gasification of forest waste with sewage sludge is that the potential to decrease the harmful substance such as sulfur, nitrogen, and alkali earth [16].

Based on the previous literature, pyrolysis and gasification can effectively deal with the sewage sludge and create environmental and economic advantages. However, studies on the production of pyrolytic oil from sewage sludge, combustion characteristics of pyrolytic oil from sewage sludge and the co-gasification of sewage sludge and forest waste are unique. Therefore, the objective is to assess the optimal production of pyrolytic oil, combustion characteristics of the blending between sludge pyrolysis oil (SPO) and heavy fuel oil (HFO), and the co-gasification of sewage sludge (SS) and forest waste using different gasification mediums.

2. METHODS

In this study, there are several biomass sources used such as a sewage sludge from a wastewater treatment plant in Tainan, Taiwan and palm kernel shell (PKS) as a forest waste from Malaysia. The sewage sludge has been dewatered by the wastewater treatment and the moisture content in the sewage sludge is around 30%. This moisture content is still high for the following experiment. Therefore, the sewage sludge was put into the oven and set the temperature to 110 ˚C until the moisture content in the sewage sludge is below 10%. Unlike the sewage sludge, the received PKS water content is already below 10%, so it is not necessary to preheat and dry the PKS in an oven. Then, sewage sludge and PKS ground pass a 100-mesh sieve for further analysis.

A thermogravimetric analysis (TGA), differential thermogravimetric analysis (DTGA), and differential scanning calorimetry analysis (DSCA) has been done using PerkinElmer STA 8000 thermal analyzer for each using a different carrier gas. In this analysis, each sample weight is 20 mg, the heating rate was set to 10 ºC/min, the carrier gas flow rate was 50 ml/min, and the temperature range was between 30 ºC to1000 ºC depending on the sample. After this pre-treatment and sample analysis, the sewage sludge will take its advantages using several experiment methods, such as the production of sludge pyrolytic oil (SPO) from sewage sludge using thermal pyrolysis apparatus; combustion characteristics of the SPO, HFO and its blending; and co-gasification of sewage sludge and PKS using different medium.

(a) (b) (c)

Figure 1: (a) sewage sludge from wastewater treatment plant (b) sewage sludge after preheating(c) palm kernel shell

2.1 Production of pyrolytic oil from sewage sludge

This experiment aimed to investigates the influence of different important parameters on the pyrolysis process of sewage sludge for producing sludge pyrolytic oil (SPO) using the Taguchi method.

2.1.1 Experimental setup

In the experiment, 90 g of dried sewage sludge was packed in a quartz tube cylindrical holder and put into the furnace, as shown in Fig.2a. Initially the tube vacuumed for pyrolysis, then the tube fill with N_2 gas to the ambient pressure. Then the furnace heat the sample to the specific temperature and maintained for a selected residence time. The heated carrier gas flow into the holder and interact with the sample. The generated volatile gas was collected and condense at 25 ◦C to produce a liquid oil. Figures 2b show pyrolysis operating process. It must undergo two steps: heated up from room to the target temperature at a specific heating rate and held at the targeted temperature for a designated residence time. The production of pyrolytic oil occurs in a certain condition and is influenced by the combination of four operational parameters: heating rate, target pyrolytic temperature, residence time, and nitrogen flow rate. The Taguchi method will analyze the influence of this parameter combination on the pyrolytic oil production from sewage sludge using a fixed-bed tubular furnace.

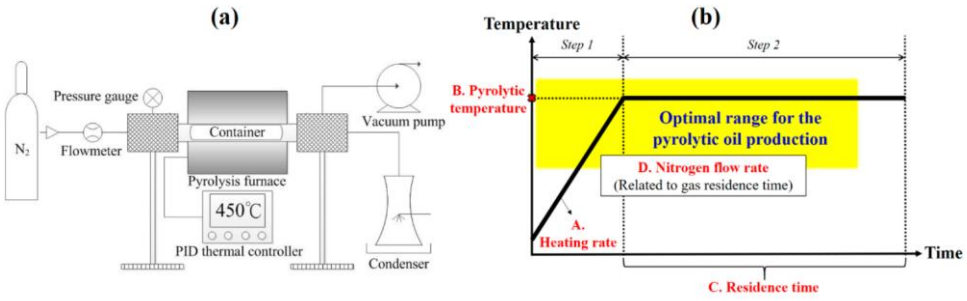

Figure 2: Schematic diagram of (a) experiment setup (b) operating process for thermal pyrolysis

2.1.2 Taguchi method

The Taguchi method was used to find the maximum yield of SPO from the pyrolysis experiments. The feature of the Taguchi method uses an orthogonal array experimental design with a simple analysis of variance. In general, the Taguchi method is not aimed at finding the optimal conditions as a full factorial method, but it can analyze the best trend with fewer experimental data and thus is commonly applied to optimize industrial processes.

Taguchi method was previously applied to analyze caster meal pyrolysis by Chen et al. and this group. The Taguchi method uses the *S*/*N* ratio, the signal to noise ratio, to measure the quality characteristics deviating from the desired value. Different strategic categories of nominal—the best (NTB), smaller the better (STB), and larger the better (L.B.)—are used to describe the *S*/*N* ratio characteristics. For example, in this study, the "larger the better" characteristic must be adopted to obtain the maximum yield of pyrolytic oil. The expression of the *S*/*N* ratio is shown as follows:

DOI: *https://doi.org/10.24036/teknomekanik.v4i2.11572*

$$S/N_{LB} = 10 \log\left(\frac{1}{N}\sum_{i=1}^{N}\frac{1}{y_i^2}\right) \quad (1)$$

Where *N* is the test number, *yi* is the value of the pyrolytic oil yield in the *i*th test. The experiment is conducted three times and take its average results.

2.2 Combustion characteristics of sewage sludge pyrolysis oil, heavy fuel oil, and their blends

The SPO is taken from the previous experiment and blended with HFO with different blending ratios. The fuel blends were mixing SPO and HFO with the pure HFO, 20% SPO/80% HFO, 40% SPO/60% HFO 60% SPO/40% HFO, 80% SPO/20% HFO and pure SPO. We used Tween 80 and Span 80 surfactants to mix the SPO and HFO, and the fuel blends were also prepared using a magnet and a magnetic stirrer.

2.2.1 Suspended droplet experiment

Fig. 3 shows the suspended droplet experiment setup used in this study. The component of this setup is a motorized stage linear guideway, two heating plates, a moving thermocouple attached in the linear guideway and a fixed thermocouple attached into the heating plate, an LED backlight, a DC power supply, a temperature controller, an electrical switch, a data collection card, a high-speed camera, and a computer. The temperature data acquired from the thermocouple and temperature controller were measured and recorded using LabVIEW software. The droplet in the linear guideway at the thermocouple was captured by the high-speed camera using a Phantom Miro C110 camera and a SIGMA MACRO 105 mm F2.8 EX DG OS HSM lens. The two heating plates had 70 mm width and 45 mm height separated by around 6.5 mm. The two plates were allowed to heat to 500ºC,550ºC, and 600ºC as the required experimental temperature. Once the required experimental temperature was reached, the LED backlight and high-speed camera were automatically turned on, and a linear guideway was moved into the gap between the heating plates to adjust the focus of the high-speed camera. The fuel droplet has a diameter of around 1000 mm at the junction of the moving thermocouples. The droplet's two-dimensional area was calculated by selecting a suitable edge detection function to discover the droplet's edge accurately. Then, the diameter of the spherical droplet could be estimated to obtain the D^2 value during the droplet heating process.

2.3 Co-gasification of sewage sludge and palm kernel shell

In this experiment, the co-gasification of sewage sludge and palm kernel shell is investigated using CO_2/steam as the gasification medium. A laboratory-scale bubbling fluidized bed gasifier with continuous feed is designed to study the co-gasification characteristics. Experiments following the Taguchi method are carried out to find the optimal operation parameters using the fluidized bed gasifier with maximum H_2/CO ratio or maximum concentration of H_2 in the syngas.

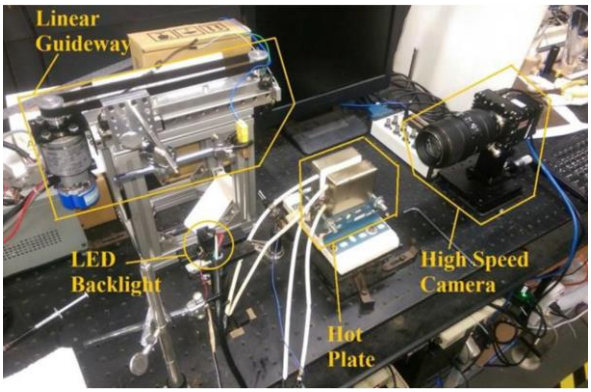

Figure 3: Suspended droplet experiment

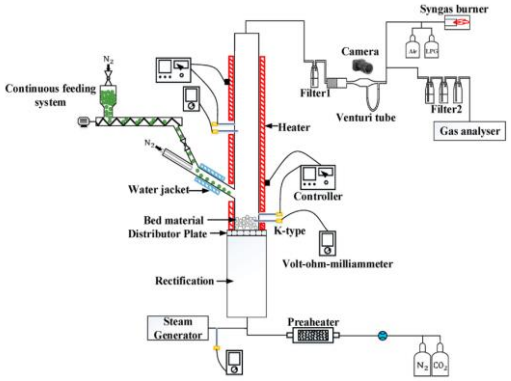

Figure 4: Fluidized bed gasifiers

2.3.1 Gasification using fluidized bed gasifier

Fig. 4 shows a schematic of the lab-scale bubbling fluidized bed gasifier (~1 kWth). It comprised several components, including a fluidized bed reactor, a gas preheater, a steam generator, a continuous feeder, an electric heater, a filtration system, a Venturi tube, a syngas analyzer (MRU VARIOluxx), and a jet burner. The fluidized bed reactor was made of a stainless (310s) cylindrical tube with a diameter of 50 mm and a height of

800 mm. The gas distributor plate was 1 mm thick and perforated with 460 holes. Fuel particle size was about 1 mm. Approximate 150 g of quartz sand (with particle sizes ranging between 250 and 300 mm) was used as the bed material in the reactor. The minimum fluidization velocity was calculated from empirical formulas. The olivine (ranging in size between 250 and 300 mm) was also added as a catalyst to promote tar reduction. The amount of catalyst is between 0% - 25% bed material mass. In this study, the operating parameters and conditions were as follows: The flow velocity was fixed at 0.225 m/s; the bed temperature ranged between 750 and 900 ºC, and the gasifying agents were steam, CO_2, or their blends.

Before the gasification experiment, the carrier gas was preheated to 500 C using a gas preheater and then passed through the gas distributor to enter the gasifier. The bed material was heated and maintained at the target temperature by the electric heater. The continuous feeder was composed of a fuel tank, a motor, a screw, stainless steel pipes, and a water jacket. The motor controlled the rotation speed of the screw, and the fuel feeding rate was fixed at 0.18 kg/h. In order to avoid heat transfer from the reactor to the fuel feeder, a water jacket was used to maintain the fuel feeder below 40 ºC. Also, a nitrogen stream was used to deliver the fuel and prevent the product gas's back-flow from the gasifier. When the gasifier temperature reached the desired value with the help of the electric heater, the hot steam produced from the steam generator was fed into the gasifier. Once the fuel had dropped into the dense phase zone in the gasifier, it was converted to syngas through the gasification process. After that, the syngas passed through the filter system and Venturi tube for gas clean-up and flowrate measurement, respectively. The venturi tube was used to estimate the syngas flow rate by a height difference of a U-shape tube. Finally, the syngas composition was detected with a gas analyzer and then was consumed using a jet burner, which has an LPG/Air flat flame for syngas burnout.

2.3.2 Taguchi method

The Taguchi method was used to find the optimal co-gasification conditions for sewage sludge and PKS. The Taguchi method in this experiment is similar to the pyrolytic oil production experiment. However, in this experiment, the Taguchi method was used to determine the maximum H_2/CO ratio and maximum H_2 concentration from the gasification; the larger better (LTB) characteristics in the Taguchi method were used. The S/N ratio for LTB is defined in Equation (1).

3. RESULTS AND DISCUSSION

This section explains the research results and, at the same time, gives a comprehensive discussion. Results can be presented in figures, graphs, tables, and others that easily understand the reader. The discussion can be made in several sub-chapters.

3.1. Production of pyrolytic oil from sewage sludge

3.1.1 Thermogravimetric Analysis of Sewage Sludge

Table 1 shows the approximate analysis of the sewage sludge used in this study, and it is composed of 6.94 wt % moisture, 45.45 wt % volatiles, 9.94 wt % fixed carbon, and 37.67 wt % ash.

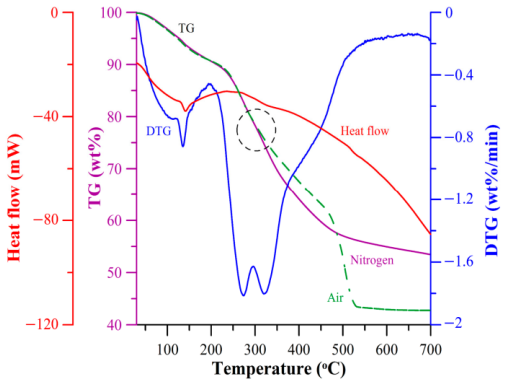

Figure 5: Thermogravimetric analysis results for sewage sludge

Figure 3 shows the TGA thermograph of sewage sludge. The heating rate is 10 ºC/min, and the nitrogen flow rate is 50 mL/min. The purple curve shows thermogravimetry (T.G.), the blue curve shows differential thermogravimetry (DTG), the red curve shows differential scanning calorimetry (DSC), while the green curve

represents T.G. in the air atmosphere. The mass loss of sewage sludge increases along with the temperature, and the major reactions occur between 120 ºC and 500 ºC

Table 1: Proximate analysis of sewage sludge

Proximate analysis	**Sewage sludge**	**Sewage sludge** [10]
Moisture (wt %)	6.94	1.5 – 7.1
Volatiles (wt %)	45.45	38.3 – 66.8
Ash (wt %)	37.67	22.6 – 52.0
Fixed carbon (wt %)	9.94	0.8 – 19.7

There are three stages of weight loss for the purple T.G. curve in Figure 5. The first stage has a weight loss of 9.33% in the temperature range of 30–200 ◦C due to removing the water and organics with low boiling points. In the second stage, there are two distinct peaks at 273 ◦C and 323 ◦C in the DTG curve. About 33.57% of the original sewage sludge is lost, and this is mainly from the decomposition of aliphatic compound protein and carbohydrates contained in the sewage sludge. In the third stage, the weight loss tends to be mild when the temperature exceeds 500 ◦C, which might be from the decomposition of residual organic matter and inorganic materials, such as calcium carbonate. Finally, the residue is about 46.79% of the original weight of the sewage sludge when the temperature reaches 1000 ◦C

3.1.1 The optimal condition for sludge pyrolysis

The optimal pyrolysis conditions for the maximum yield SPO are investigated using the Taguchi method in the fixed bed reactor. The table gives the parameters and their levels. Four pyrolysis parameters are the heating rate, pyrolysis temperature, residence time, and nitrogen flow rate. These parameters are assumed to be independent, and each parameter has four levels. Table 2 shows the experimental layout and the mass balance of all experimental conditions, including aqueous, oil, and solid yields from the calculation. Each experiment was performed three times and took the average to assure the reliability of the results.

Table 2: Experimental layout and mass balance

Experiment No.	**Experimental layout**				**Mass Balance**			
	HR (ºC/min)	**T (ºC)**	**RT (min)**	**N_2 (mL/min)**	**Aqueous (wt%)**	**Oil (wt%)**	**Solid (wt%)**	**Gas (by diff.) (wt%)**
1	10	450	30	300	11.42	8.71	57.02	22.85
2	10	500	60	500	12.67	8.88	55.09	23.36
3	10	550	90	700	15.06	9.87	54.48	20.60
4	10	600	120	900	13.42	7.29	52.18	27.11
5	20	450	30	300	14.93	8.76	54.92	21.40
6	20	500	60	500	14.09	7.91	53.37	24.63
7	20	550	90	700	14.31	8.62	52.45	24.62
8	20	600	120	900	9.44	9.22	54.10	27.24
9	30	450	30	300	13.41	8.31	55.80	22.49
10	30	500	60	500	12.12	9.32	54.56	24.00
11	30	550	90	700	12.93	6.59	53.10	27.38
12	30	600	120	900	13.76	7.58	52.91	25.75
13	40	450	30	300	14.70	9.20	54.43	21.66
14	40	500	60	500	13.11	5.43	54.30	27.17
15	40	550	90	700	18.41	9.22	53.33	19.03
16	40	600	120	900	15.67	7.88	51.82	24.63

After obtaining the experimental yield of SPO, the corresponding *S*/*N* ratio can be calculated using Equation (1). The mean *S*/*N* ratio for the 16 experimental conditions is computed, and the mean *S*/*N* ratio for each level of the other pyrolysis parameters can then be calculated.

The optimal operation conditions are determined based on the experimental results and the calculated S/N ratio, as shown in Fig. 6. In Fig. 6, these four pyrolysis parameters are labelled as "A" for heating rate, "B" for pyrolytic temperature, "C" for residence time, and "D" for nitrogen flow rate. It can be deduced from Figure 6 that the optimal pyrolysis conditions are A1, B1, C2, and D3, which represent a heating rate of 10 C/min, the

pyrolytic temperature of 450 ◦C, the residence time of 60 min, and nitrogen flow rate of 700 mL/min. The results show that oil yield was affected by the combination of four operational parameters. The nitrogen flow rate has the most obvious effect among these parameters, followed by the pyrolytic temperature, heating rate, and residence time.

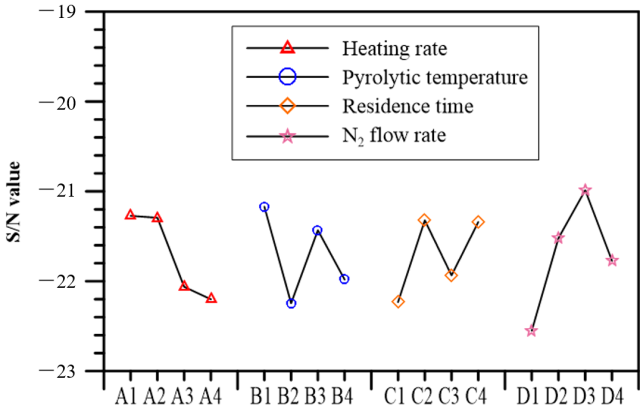

Figure 6: S/N response for SPO

In the Taguchi method, the confirmation experiment is the last step, and the aim is to validate the yield of SPO. After obtaining the optimum conditions and predicting the response under these conditions, a new experiment was performed with the optimum levels of these pyrolysis parameters. The theoretical optimal *S*/*N* ratio can be estimated as:

$$S/N_{opt} = S/N_{Av} + \left(A1 - S/N_{Av}\right) + \left(B1 - S/N_{Av}\right) + \left(C2 - S/N_{Av}\right) + \left(D3 - S/N_{Av}\right) \quad (2)$$

From the experimental results, the theoretical optimization *S*/*N* value is -19.63, and it can be deduced that the theoretical maximum pyrolytic oil yield is 0.1044 g/g-sewage sludge (18.85% on a dry ash-free (daf) basis). The real yield of the confirmation experiment is 0.1019 g/g-sewage sludge (18.4% on a dry ash-free (daf) basis). The difference is only 0.0025 g/g sewage sludge, and the thus real experimental result is very close to the theoretical value. In addition, under the optimal conditions, the solid product is about 54.83%, the aqueous product is about 15%, and the gas product is 19.98% by mass balance.

3.2. Combustion characteristics of sewage sludge pyrolysis oil, heavy fuel oil, and their blends

3.2.1 Thermogravimetric analysis of SPO and HFO

Fig. 7a shows the TGA results for the SPO fuel. The weight loss curve contains three important stages. Stage 1 is the moisture evaporation stage ranging from 30 ºC to 134 ºC. The DTG curve has peaks at 105 ºC and 115 ºC, and an endothermic reaction is indicated by the DSC curve. Stage 2 is the volatile decomposition and burning stage, with temperatures ranging from 134 ºC to 485 ºC. The released components include lightweight components (LWC) and middleweight components (MWC). The DSC curve shows a slight exothermic reaction between 300 ºC and 450 ºC, with a peak at a temperature of 395 ºC. It is speculated that the combustion heat released during this period results from volatile burning. In addition, the total weight loss was approximately 77.19 wt%. Stage 3 is the primary combustion stage at temperatures higher than 485 C. In this stage, the DTG curve had a significant peak at 624 ºC due to further decomposition of the HWC, which subsequently reacted with the oxygen and exhibited an intense release of combustion heat. Finally, the total weight loss in this stage was approximately 11.90 wt%, with almost no remaining residue.

Fig. 7b shows the TGA results for the HFO. The weight loss curve comprises only two main regions in the HFO. The moisture evaporation stage (stage 1) of the HFO is vague due to the very low moisture content in the HFO. Stage 2 is the volatile decomposition and burning stage, with temperatures ranging from 30 ºC to 582 ºC. Initially, the DSC curve remains approximately constant until 287 ºC. A noticeable exothermic peak occurs at 359 ºC, indicating a volatile burning heat release. The DTG curve has a peak located at 354 ºC. At higher temperatures, the DTG curve shows another peak. The second peaks at 396 ºC indicate the primary endothermic reaction, and the last two peaks are located at 467 ºC and 485 C, respectively. Stage 3 is the combustion stage, with temperatures higher than 525 ºC. The DTG curve shows a significant peak at 671 ºC and shows an intense combustion heat release for the DSC curve. The exothermic reactions result from the

DOI: *https://doi.org/10.24036/teknomekanik.v4i2.11572*

further decomposition and burning of the high weight component (HWC). The total weight loss is approximately 10.21 wt%.

Fig. 7c and 7d show the TGA results for the different SPO/ HFO fuel blends. As shown, the weight loss in the moisture evaporation stage increases with increases in the SPO content due to high moisture content in the HFO. In the early volatile decomposition and burning stage, the fuel blend with a higher SPO content shows a more significant weight loss rate than the higher HFO content. However, the weight loss increases significantly in the higher HFO content in the high-temperature region. The higher LWC content mainly causes this result in the SPO compared with HFO, and these LWC components vaporize easier in the lower temperatures. Since the HFO contain more MWC, some MWC is released near the end of the volatile decomposition and burning stage, which cause more intense weight loss than is the case for SPO.

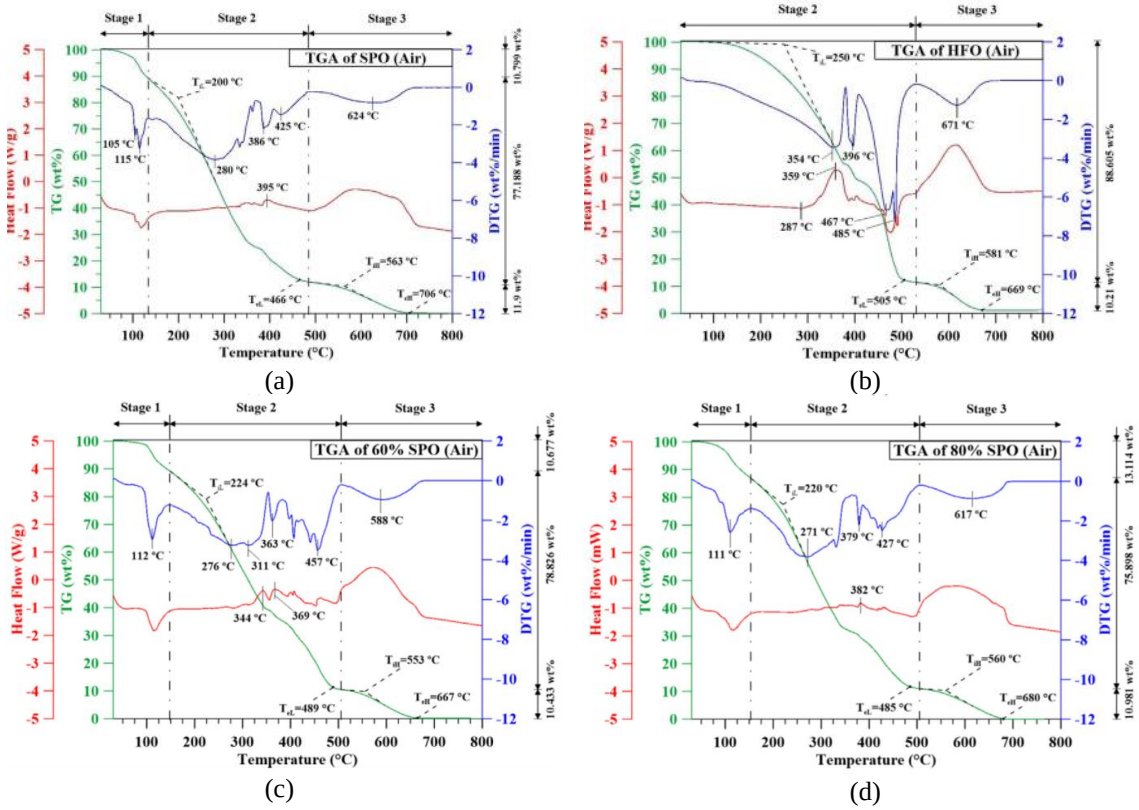

Figure 7: Thermogravimetric analysis of the SPO/HFO blends (a) Pure SPO (b) Pure HFO (c) 60% SPO/ 40% HFO (d) 80% SPO/ 20% HFO

3.2.2 Suspended droplet experiments

In general, various stages can be observed during the suspended droplet experiments, and these stages can be described as follows:

(i) **The surface micro-explosion stage:** The LWC near the surface is vaporized and nucleated. The LWC induces a continuous micro explosion with a low intensity that distorts the droplet shape.

(ii) **The interior micro-explosion stage:** The LWC in the droplet's interior becomes superheated. When the superheating limit is exceeded, homogeneous nucleation and vaporization occur, resulting in an accumulation of pressure within the droplet. This pressure causes swelling or expansion of the droplet, leading to the droplet being pulled into smaller droplets, broken into pieces, or released as fuel oil vapour into the ambient environment.

(iii) **The vaporization stage:** The droplet boiling point is governed mainly by the MWC. However, if the ambient temperature is not excessively high, the MWC near the droplet surface may be vaporized with the LWC in the droplet's interior. The pressure accumulated within the droplet is lower than in the

interior micro-explosion stage. Consequently, the surface micro-explosion and interior micro explosion's intensity is reduced, and droplet shrinkage occurs.

(iv) The expansion micro-explosion stage: If the ambient temperature is very high, the MWC near the droplet surface and the LWC in the droplet's interior are heated rapidly and vaporized. The resulting pressure accumulation within the droplet is like that in the interior micro-explosion stage. However, the magnitude of the accumulated pressure is greater. Consequently, high-intensity expansion and an explosion occur, leading to a dramatic distortion in the droplet shape. It should be noted that the expansion micro explosion stage always precedes the combustion stage.

(v) The combustion stage: The released fuel vapor mixes with the oxygen in the environment and is ignited if the ambient temperature is sufficiently high. The resulting flame propagates from the surroundings to the main droplet and forms a non-premixed flame that wraps around the main droplet. This combustion event increases the heating rate of the droplet and the intensity of the micro-explosion. As a result, a dramatic distortion in the droplet shape occurs, which results in the release of fuel oil vapor and therefore enhances the existing flame. The combustion process proceeds continuously until all the volatile components in the droplet are consumed.

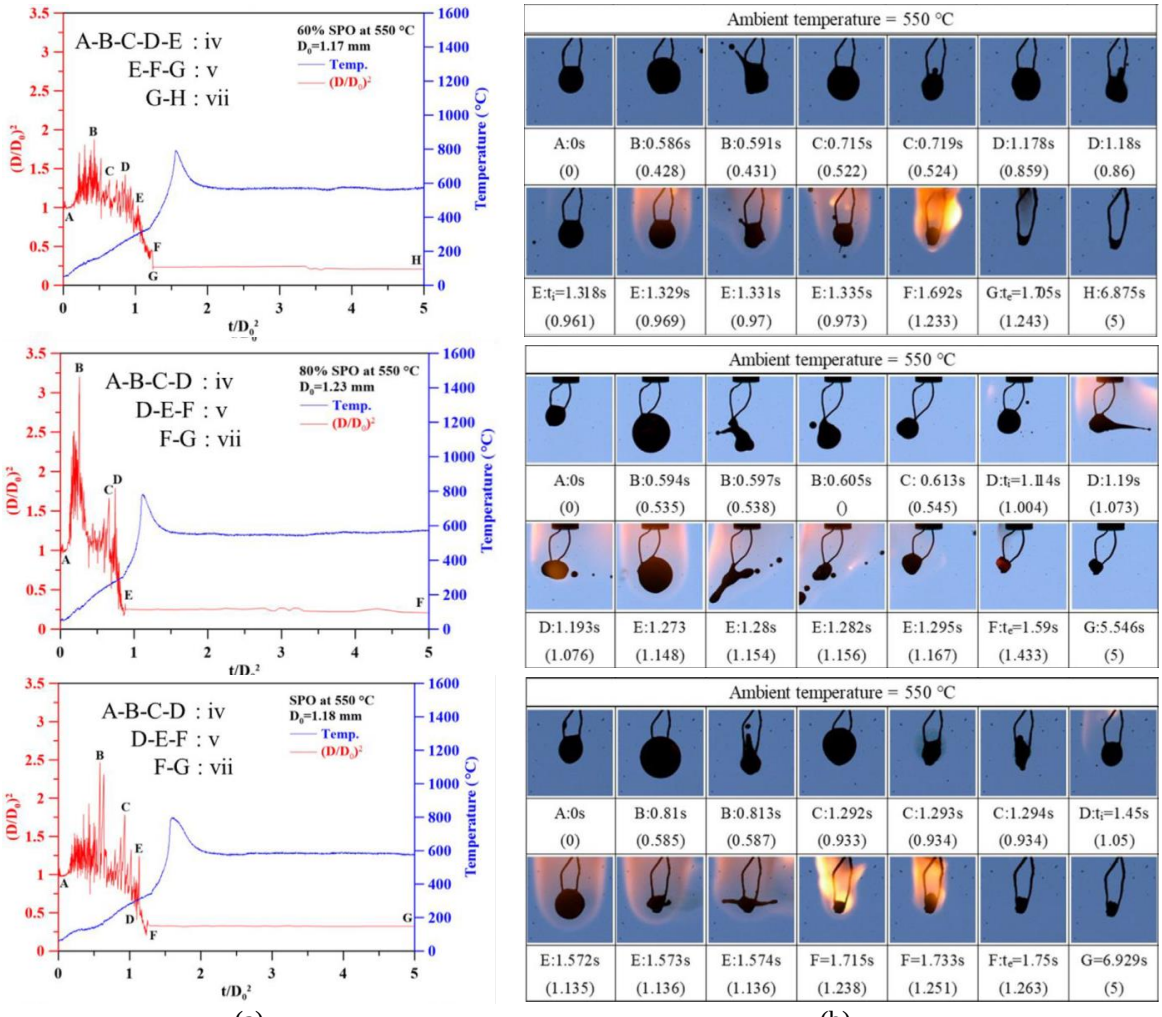

(a) (b)

Figure 8: (a) Variations in the droplet size for the 60%, 80%, 100% SPO fuel blend at different temperatures, (b) Droplet heating processes for the 60%, 80%, 100% SPO fuel blend at different temperatures.

(vi) The smolder stage: Following the combustion stage, the volatile components in the droplet are completely burned. However, the combustible solid particles continue to burn. While no

obvious flame exists, the solid residue is red or orange, gradually extinguishing as the solid particles are burned.

(vii) The residual stage: The **ambient** temperature is not high enough to vaporize the droplet, ignite the fuel vapor surrounding the droplet, or burn out the remaining combustible solid particles. The residual product is typically a liquid phase, solid phase, or sludge-like phase.

Fig. 8 show the results for the suspended droplet experiment for the SPO/HFO fuel blends with ambient temperature of 550ºC at different blending ratios, where (a) the change in the droplet size during the heating or combustion period, and (b) shows the image sequence of the droplet at ambient temperatures of 550 C. The other stages are also marked on the figures to indicate the various heating behaviors. For the fuel blends with 60% SPO, this stage occurred in period A-B-C-D-E (0 - 1.335 s); the 80% SPO fuel blend and pure SPO occurred in period A-B-C-D (0 - 1.193 s and 0 - 1.45 s), respectively. Overall, the results showed that the intensity of the micro-explosion event increased with an increase in the SPO content.

The fuel blends with a higher SPO ratio (i.e., 60 - 80% SPO and pure SPO) exhibited a combustion stage in period E-F-G (1.329 - 1.705 s) for the 60% SPO fuel blends and in period D-E-F (1.114 - 1.59 s and 1.45 - 1.75 s) for the 80% SPO fuel blend and pure SPO fuel, respectively. Finally, all the fuels exhibited a residual stage. The residual product of the fuel blends with a higher SPO content (i.e., 60 - 80% SPO and pure SPO) ranged in size between 0.18 - 0.43 times that of the original diameter

Table 3: Heating performance of the different SPO/HFO fuel blends in the different ambient temperature

SPO %	Temperature	Surface micro-explosion	Interior micro-explosion	Vaporization	Expansion micro-explosion	Combustion	Smolder	Residue
0	500 °C	○	○					○
20		○	○					○
40		○	○					○
60		○	○					○
80				●	○			○
100				●	○			○
0	550 °C	○	○					○
20		○	○					○
40		○	○					○
60					○	●		○
80					○	●		○
100					○	●		○
0	600 °C	○				○		○
20					○	●		○
40					○	●		○
60					○	●	○	○
80					○	●	○	○
100					○	●	○	○

●: vaporization/combustion rate can be approximated using a linear regression analysis

3.2.3 Combustion rate

All the single droplet heating behaviors for the different SPO/HFO blends are summarized in table 3. We can see that in there is no combustion happen in the ambient temperature of 500ºC. Some blending indicates that the changes in the droplet size can be approximated by a straight line using a linear regression analysis

technique with the least square error in the ambient temperature of 550ºC and 600ºC. The slope of this straight line represents the vaporization or combustion rate.

Fig. 9 shows a suspended droplet experiment results for the fuel blend with different SPO/HFO ratios at an ambient temperature of 550 C. The figure also shows that the linear regression line indicates the combustion rate. The 60% SPO fuel blend had a combustion rate approximately of 2.226 mm^2/s over the range of t/D_0^2 = 0.961 - 1.243. The 80% SPO fuel blend had a combustion rate approximately of 2.556 mm^2/s over the range of t/D_0^2 = 1.004 - 1.433, while the pure SPO fuel had a combustion rate approximately of 3.047 mm^2/s over the range of t/D_0^2 = 1.05 - 1.263. Higher SPO content increased the combustion rate of the fuel blends. Since sludge pyrolysis oil contains higher moisture, the water evaporates at the beginning of the combustion process leading to a longer ignition delay. The ignition delay time increased with the increment of SPO.

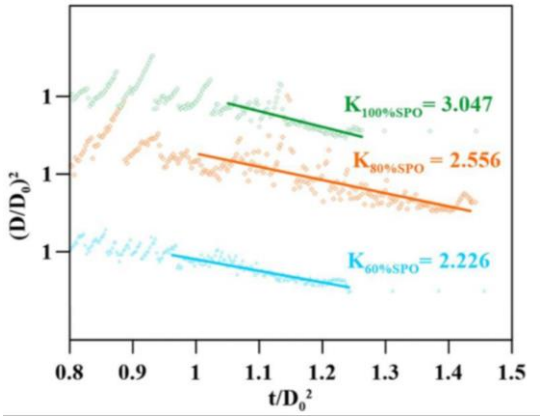

Figure 9: Experimental results for suspended droplets

3.3. Co-gasification of sewage sludge and palm kernel shell

3.3.1 Thermogravimetric analysis

Fig. 10a shows T.G. and DTG curves of pure PKSs in N_2 and CO_2 environments, where four stages of weight loss occur. The first stage ended at 169 ºC due to the weight loss from some remaining moisture content in the PKS. The second and third stages, which ended at 321 ºC and about 400 ºC were denoted as the pyrolysis of hemicellulose and cellulose, respectively. The final stage may have been the pyrolysis of lignin. It is worth noting that when PKS is in a CO_2 environment, the fourth-stage thermal decomposition occurs earlier and has a higher weight loss rate. Fig. 10b shows the TG and DTG curves of pure sewage sludge in N_2 and CO_2 environments. Weight loss can be divided into three stages. The first stage ended near 181 C, and all the moisture had evaporated. The second stage ended at about 589 ºC. It was speculated that the thermal decomposition of lipids, cellulose, and protein occurred in this temperature range. The last stage was the thermal decomposition of heavyweight components or inorganic matter. In a CO_2 environment, the overall weight loss rate is enhanced, and the reaction is also completed earlier.

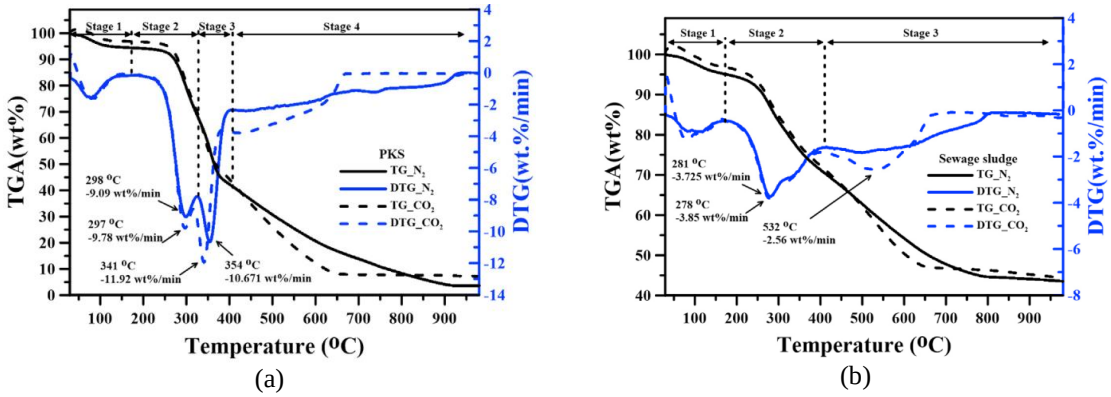

(a) (b)

Figure 10: The T.G. and DTG results for PKS (a) and sewage sludge (b) under N_2 and CO_2 environments,

DOI: https://doi.org/10.24036/teknomekanik.v4i2.11572

Table 4: Experiment Layout and gas composition

Experiment No.	Experimental layout				Gas Composition				
	T (°C)	BR (%)	$CO_2/(CO_2+H_2O)$ (%)	Catalyst (%)	CO2 (%)	CO (%)	H2 (wt%)	CH4 (%)	N2 (%)
1	750	0	55	0	39.2	28.3	6.5	4.1	19.9
2	750	20	70	15	59	14.3	5.7	1.5	18.3
3	750	30	85	20	59.7	13.7	6.0	4.8	14.6
4	750	40	100	25	67	12.7	2.3	1.2	18.3
5	800	0	55	0	38.5	32.0	13.7	3.4	12.3
6	800	20	70	15	49.5	18.0	9.5	1.7	21.3
7	800	30	85	20	56.3	19.4	3.7	1.8	18.8
8	800	40	100	25	62.8	13.3	4.8	1.2	18.0
9	850	0	55	0	52.2	24.7	7.5	1.8	13.9
10	850	20	70	15	41.4	33.7	7.1	4.1	13.7
11	850	30	85	20	52.4	16.1	7.7	1.7	22.1
12	850	40	100	25	57.6	14.3	6.1	1.8	20.0
13	900	0	55	0	32.6	37.7	9.6	5.3	14.8
14	900	20	70	15	53.1	22.1	6.0	4.0	14.8
15	900	30	85	20	55.0	17.1	7.9	1.5	18.5
16	900	40	100	25	49.7	18.5	9.3	1.7	20.8

3.3.2 The optimal conditions for co-gasification of SS and PKS in the fluidized bed gasifier

In general, the temperature is one of the most crucial parameters in gasification, and it is usually located between 750 and 900 °C. It also dominates the char reaction rate, gasifier efficiency, secondary cracking of tar, and pollutant formation during gasification. In addition, the gasifying medium, such as Air, CO_2, and H_2O, can alter the H_2/CO ratio of syngas, where, especially, CO_2 and H_2O can react with char and tar and generate more combustible gas. The effects of gasification temperature, the fuel blending ratio, $CO_2/(CO_2+H_2O)$ ratio, and catalyst addition on the H_2/CO ratio and H_2 concentration were investigated with the Taguchi method in a fluidized bed gasifier. These are important parameters in the practical operation of the gasifier. Moreover, some parameters were fixed for all cases, such as the fluidization velocity of 0.225 m/s (5 L/min), the fuel feeding rate of 0.18 kg/h, and the bed material (150 g). In addition, olivine was used as an additive catalyst with different weights relative to the bed material.

The gas compositions obtained in the 16 experiments are shown in Table 4. The experimental results are used to calculate the corresponding S/N ratios using Equation (1) to obtain the maximum H_2/CO ratio and maximum H_2 concentration. The optimum theoretical value could be predicted by substituting the S/N ratio of the parameters at optimal levels into Equation (2)

Table 5: S/N Response table for H_2/CO ratio and max H_2 concentration

	H_2/CO ratio					Max H_2 concentration				
	L1	L2	L3	L4	max-min	L1	L2	L3	L4	max-min
T (°C)	-10.3	-9.05	-9.25	-9.00	2.35	-14.00	-12.39	-12.59	-12.53	1.61
BR (%)	-10.64	-9.06	-8.69	-9.25	1.95	-13.72	-12.63	-12.58	-12.57	1.15
$\frac{CO_2}{CO_2+H_2O}$ (%)	-7.69	-6.98	-9.50	-13.4	6.42	-11.46	-10.84	-13.25	-15.96	5.12
Catalyst (%)	-11.52	-8.41	-8.37	-9.35	3.15	-14.6	-11.94	-12.39	-12.57	2.66

Table 5 shows the optimal operation conditions were obtained using the analytical results for the mean S/N ratio. From the table, we can see that the maximum H_2/ CO ratio reach with the gasification temperature of 900 C, a blending ratio of 30%, a $CO_2/(CO_2+H_2O)$ ratio of 70%, and a catalyst addition of 20% bed material mass. The maximum concentration of H_2 was 32.2% with gasification temperature of 800 C, a blending ratio of 40%, a $CO_2/(CO_2+H_2O)$ ratio of 70%, and a 15% catalyst addition of bed material mass. In the H_2/CO ratio, the $CO_2/(CO_2+H_2O)$ ratio is the most significant variable, followed by catalyst addition, blending ratio, and finally, gasification temperature. The S/N ratio at the optimal level (S/N_{opt}) for H_2/CO ratio was 4.81, and the obtained maximum H_2/CO ratio was 0.574. The confirmation experiment was then performed, and the result

revealed that the maximum H_2/CO ratio was 0.563, which was only a 0.011 difference from the theoretical value. In the case of maximum H_2 concentration, CO_2/ (CO_2+H_2O) ratio was the most significant parameter, followed by catalyst addition, gasification temperature, and finally, the blending ratio. The calculated S/N_{opt} ratio was 9.13, and the maximum concentration of H_2 was 34.9%. The experimental confirmation results showed a value of 32.2% for the normalized H_2 concentration.

4. CONCLUSION

The optimal production of pyrolytic oil, combustion characteristics of the blending between sludge pyrolysis oil (SPO) and heavy fuel oil (HFO) with different blending ratios and co-gasification of sewage sludge (SS) and palm kernel shell (PKS) using different gasification mediums was investigated. The findings of this study are summarized as follow:

(1) The effective sequence of pyrolytic parameters for the yield of sludge pyrolytic oil is nitrogen flow rate, pyrolytic temperature, heating rate, and residence time. The best operating conditions for sewage sludge pyrolysis are a heating rate of 10 ◦C/min, pyrolysis temperature of 450 ◦C, residence time of 60 min, and nitrogen flow rate of 700 mL/min. Under these conditions, the obtained pyrolytic oil yield is 10.19% (18.4% on dry ash free (daf) basis), which is very close to 10.44% (18.85% on dry ash free (daf) basis.), the ideal value from the Taguchi method.

(2) Various stages can be observed in the suspended droplet experiments for SPO/HFO blends, including (i) a surface micro explosion stage, (ii) an interior micro-explosion stage, (iii) a vaporization stage, (iv) an expansion micro-explosion stage, (v) a combustion stage, (vi) a smolder stage, and (vii) a residual stage. SPO contains a higher amount of water and LWC than HFO. Therefore, a higher SPO content in the fuel blend increases the frequency of micro-explosion and reduces the size of the residual product. An ambient temperature of 550 C with more than 60% SPO shows almost constant combustion rates. Higher SPO content in the fuel blend increases the combustion rate and the ignition delay time due to the moisture evaporation process.

(3) Using the Taguchi method, different operating parameters, such as gasification temperature, the fuel blending ratio, the CO_2/(CO_2+H_2O) ratio, and catalyst addition were investigated. The optimal operating conditions necessary to obtain the maximum H_2/ CO ratio and the maximum H_2 concentration in the bubbling fluidized bed gasifier were obtained. The maximum H_2/ CO ratio reach with the gasification temperature of 900 C, a blending ratio of 30%, a CO_2/(CO_2+H_2O) ratio of 70%, and a catalyst addition of 20% bed material mass. The maximum concentration of H_2 reach with gasification temperature of 800 C, a blending ratio of 40%, a CO_2/(CO_2+H_2O) ratio of 70%, and a 15% catalyst addition of bed material mass. Hydrogen is a promising energy carrier with large energy density and the hydrogen-rich syngas could help minimize the CO_2 equivalent emission. The CO_2/(CO_2+H_2O) ratio was always the dominant parameter in the selected conditions in the study. In addition, catalyst addition was the second dominant effect on the maximum H_2/CO ratio and maximum H_2 concentration. The amount of catalyst with 15 - 20% bed material mass had the significant effect in this study. These experimental results of the 1 kWh continuous type fluidized-bed gasifier could be used as a reference for the practical operation of the large-scale gasifier.

REFERENCES

[1] G. B. Chen, Y. H. Li, T. S. Cheng, and Y. C. Chao, "Chemical effect of hydrogen peroxide addition on characteristics of methane-air combustion," *Energy*, vol. 55, pp. 564–570, Jun. 2013, doi: 10.1016/j.energy.2013.03.067.

[2] A. Starikovskiy and N. Aleksandrov, "Plasma-assisted ignition and combustion," *Prog. Energy Combust. Sci.*, vol. 39, no. 1, pp. 61–110, 2013, doi: 10.1016/j.pecs.2012.05.003.

[3] W. Kaminski, J. Marszalek, and A. Ciolkowska, "Renewable energy source-Dehydrated ethanol," *Chem. Eng. J.*, vol. 135, no. 1–2, pp. 95–102, 2008, doi: 10.1016/j.cej.2007.03.017.

[4] P. S. Nigam and A. Singh, "Production of liquid biofuels from renewable resources," *Prog. Energy Combust. Sci.*, vol. 37, no. 1, pp. 52–68, 2011, doi: 10.1016/j.pecs.2010.01.003.

[5] J. Werther and T. Ogada, "Sewage sludge combustion," *Prog. Energy Combust. Sci.*, vol. 25, no. 1,

pp. 55–116, 1999, doi: 10.1016/S0360-1285(98)00020-3.
[6] S. M. Al-Salem, A. Antelava, A. Constantinou, G. Manos, and A. Dutta, "A review on thermal and catalytic pyrolysis of plastic solid waste (PSW)," *J. Environ. Manage.*, vol. 197, no. 1408, pp. 177–198, 2017, doi: 10.1016/j.jenvman.2017.03.084.
[7] A. P. Bora, D. P. Gupta, and K. S. Durbha, "Sewage sludge to bio-fuel: A review on the sustainable approach of transforming sewage waste to alternative fuel," *Fuel*, vol. 259, no. October 2019, p. 116262, 2020, doi: 10.1016/j.fuel.2019.116262.
[8] Z. Wang *et al.*, "Co-pyrolysis of sewage sludge and cotton stalks," *Waste Manag.*, vol. 89, pp. 430–438, 2019, doi: 10.1016/j.wasman.2019.04.033.
[9] A. Zaker, Z. Chen, X. Wang, and Q. Zhang, "Microwave-assisted pyrolysis of sewage sludge: A review," *Fuel Process. Technol.*, vol. 187, no. February, pp. 84–104, 2019, doi: 10.1016/j.fuproc.2018.12.011.
[10] T. Lu, H. R. Yuan, S. G. Zhou, H. Y. Huang, K. Noriyuki, and Y. Chen, "On the pyrolysis of sewage sludge: The influence of pyrolysis temperature on biochar, liquid and gas fractions," *Adv. Mater. Res.*, vol. 518–523, pp. 3412–3420, 2012, doi: 10.4028/www.scientific.net/AMR.518-523.3412.
[11] I. Fonts, G. Gea, M. Azuara, J. Ábrego, and J. Arauzo, "Sewage sludge pyrolysis for liquid production: A review," *Renew. Sustain. Energy Rev.*, vol. 16, no. 5, pp. 2781–2805, 2012, doi: 10.1016/j.rser.2012.02.070.
[12] D. B. Spalding, "Experiments on the burning and extinction of liquid fuel spheres," *Fuel*, vol. 32, no. 2, pp. 169–185, 1953.
[13] S.-W. Kang, J.-I. Dong, J.-M. Kim, W.-C. Lee, and W.-G. Hwang, "Gasification and its emission characteristics for dried sewage sludge utilizing a fluidized bed gasifier," *J. Mater. Cycles Waste Manag.*, vol. 13, no. 3, pp. 180–185, 2011, doi: 10.1007/s10163-011-0016-y.
[14] A. A. Oladejo, M. O. Oyama, K. O. Ayeni, E.-O. Ayo, and A. S. Oyerinde, "In vitro Evaluation of Antibacterial and Antifungal Activities of Chrysophyllum albidum Stems Bark," *J. Adv. Microbiol.*, vol. 13, no. 2, pp. 1–7, 2018, doi: 10.9734/jamb/2018/32983.
[15] M. C. Samolada and A. A. Zabaniotou, "Comparative assessment of municipal sewage sludge incineration, gasification and pyrolysis for a sustainable sludge-to-energy management in Greece," *Waste Manag.*, vol. 34, no. 2, pp. 411–420, 2014, doi: 10.1016/j.wasman.2013.11.003.
[16] A. Ramos, E. Monteiro, V. Silva, and A. Rouboa, "Co-gasification and recent developments on waste-to-energy conversion: A review," *Renew. Sustain. Energy Rev.*, vol. 81, no. June 2016, pp. 380–398, 2018, doi: 10.1016/j.rser.2017.07.025.

NOMENCLATURE

SS	Sewage sludge
PKS	Palm kernel shell
SPO	Sludge pyrolysis oil
HFO	Heavy fuel oil
S/N	Signal to noise ratio
DSC	Digital scanning calorimetry
TG	Thermogravimetric
DTG	Differential thermogravimetric
LTB	Larger the better
HR	Heat rate
T	Temperature
RT	Residence time
LWC	Light weight component
MWC	Medium weight component
HWC	High weight component
BR	Blending ratio
T_i	Ignition temperature
T_e	Extinction temperature